Check for updates

The enzymatic activity of 5-aminoimidazole-4-carboxamide ribonucleotide formyltransferase/IMP cyclohydrolase is enhanced by NPM-ALK: new insights in ALK-mediated pathogenesis and the treatment of ALCL

*Francesco E. Boccalatte,[1,2] *Claudia Voena,[1,2] Chiara Riganti,[1,3] Amalia Bosia,[1,3] Lucia D'Amico,[1,2] Ludovica Riera,[1,2] Mangeng Cheng,[4] Bruce Ruggeri,[4] Ole N. Jensen,[5] Valerie L. Goss,[6] Kimberly Lee,[6] Julie Nardone,[6] John Rush,[6] Roberto D. Polakiewicz,[6] Michael J. Comb,[6] Roberto Chiarle,[1,2] and Giorgio Inghirami[1,2,7]

[1]Center for Experimental Research and Medical Studies (CERMS), [2]Department of Biomedical Sciences and Human Oncology, and [3]Department of Genetics, Biology, and Biochemistry, University of Torino, Torino, Italy; [4]Discovery Research, Cephalon, West Chester, PA; [5]Department of Biochemistry and Molecular Biology, University of Southern Denmark, Odense, Denmark; [6]Cell Signaling Technology, Danvers, MA; and [7]Department of Pathology and New York University Cancer Center, New York University School of Medicine, New York

Anaplastic large cell lymphoma represents a subset of neoplasms caused by translocations that juxtapose the anaplastic lymphoma kinase (ALK) to dimerization partners. The constitutive activation of ALK fusion proteins leads to cellular transformation through a complex signaling network. To elucidate the ALK pathways sustaining lymphomagenesis and tumor maintenance, we analyzed the tyrosine-kinase protein profiles of ALK-positive cell lines using 2 complementary proteomic-based approaches, taking advantage of a specific ALK RNA interference (RNAi) or cell-permeable inhibitors. A well-defined set of ALK-associated tyrosine phosphopeptides, including metabolic enzymes, kinases, ribosomal and cytoskeletal proteins, was identified. Validation studies confirmed that vasodilator-stimulated phosphoprotein and 5-aminoimidazole-4-carboxamide ribonucleotide formyltransferase/inosine monophosphate cyclohydrolase (ATIC) associated with nucleophosmin (NPM)–ALK, and their phosphorylation required ALK activity. ATIC phosphorylation was documented in cell lines and primary tumors carrying ALK proteins and other tyrosine kinases, including TPR-Met and wild type c-Met. Functional analyses revealed that ALK-mediated ATIC phosphorylation enhanced its enzymatic activity, dampening the methotrexate-mediated transformylase activity inhibition. These findings demonstrate that proteomic approaches in well-controlled experimental settings allow the definition of informative proteomic profiles and the discovery of novel ALK downstream players that contribute to the maintenance of the neoplastic phenotype. Prediction of tumor responses to methotrexate may justify specific molecular-based chemotherapy. (Blood. 2009;113:2776-2790)

Introduction

Cell transformation is the result of the sequential acquisition of multiple genetic defects, which provide a growth and survival advantage to the cancerous cells and the acquisition of metastatic potential.[1] The activation of oncogenes and the loss of tumor suppressor genes are pivotal in cancer development, as they deregulate multiple metabolic pathways and contribute to the neoplastic phenotype. Better understanding of key metabolic checkpoints in cancer cells would allow the design of novel therapeutic strategies. Dividing cells heavily rely on de novo purine synthesis, whereas normal cells prefer the salvage pathway.[2] Glycinamide ribonucleotide formyltransferase and the bifunctional 5-aminoimidazole-4-carboxamide ribonucleotide (AICAR) formyltransferase/inosine monophosphate (IMP) cyclohydrolase (AICAR-FT/IMP-CHase, named ATIC) have raised considerable attention because of their role in cancer. Both enzymes are folate-dependent and have become exquisite targets of chemotherapeutic intervention.[2-4]

ATIC is a bifunctional enzyme that catalyzes the final 2 steps of de novo purine biosynthesis pathway.[3-5] The AICAR formyltransferase (AICAR-FT) domain (residues 199-592) catalyzes the transfer of the one-carbon formyl group from the cofactor N^{10}-formyl-tetrahydrofolate (10-f-THF) to the substrate AICAR to produce N-formyl-5-aminoimidazole-4-carboxamide ribonucleotide (F-AICAR) and tetrahydrofolate. The IMP cyclohydrolase domain (IMP-Chase; residues 1-198) then enhances the intramolecular cyclization of N-formyl-AICAR to the final product of the pathway, IMP.[6]

The *ATIC* gene is fused, as result of cryptic inversion [inv(2)(9p23q35)], to the anaplastic lymphoma kinase (*ALK*) in a subset of anaplastic large cell lymphoma (ALCL). ALCL, a distinct entity among T-cell non-Hodgkin lymphoma (NHL), is a hematologic disorder that accounts for approximately 30% of all pediatric NHLs. Many ALCLs carry translocations that involve *ALK* and variable partner genes (mainly nucleophosmin [NPM1]). In ATIC-ALK, the N-terminus of ATIC fuses to the intracytoplasmic region of ALK and encodes a novel oncogenic chimeric protein.[7-9]

ALK chimeras have constitutive tyrosine kinase activity with oncogenic potential. In vitro and in vivo studies have demonstrated

Submitted June 3, 2008; accepted August 9, 2008. Prepublished online as *Blood* First Edition paper, October 9, 2008; DOI 10.1182/blood-2008-06-161018.

*F.E.B. and C.V. contributed equally to this manuscript.

An Inside *Blood* analysis of this article appears at the front of this issue.

The online version of this article contains a data supplement.

The publication costs of this article were defrayed in part by page charge payment. Therefore, and solely to indicate this fact, this article is hereby marked "advertisement" in accordance with 18 USC section 1734.

© 2009 by The American Society of Hematology

Downloaded from http://ashpublications.net/blood/article-pdf/113/12/2776/1305103/zh801209002776.pdf by guest on 20 May 2024

that ALK signaling induces cell transformation by modulating many adaptor proteins involved in cell-cycle progression, survival, cytoskeletal rearrangement, and cell migration.[10] ALK signaling is required and necessary to maintain the neoplastic phenotype because the loss of ALK activity causes cell-cycle arrest and cell death in vitro, and tumor regression in vivo.[11,12] These findings have fostered the discovery of ALK small-molecule inhibitors that are now in early clinical trials or on the verge of entering the clinical arena. The discovery that deregulated expression of ALK can be seen in a subset of nonhematologic tumors, including inflammatory myofibroblastic tumors, non–small cell lung cancer, sarcoma, and neuroblastoma,[12] has increased the interest on ALK, as a promising target for specific therapies.

Because some signaling molecules essential for ALK-mediated transformation[10] display a key function in other ALK$^-$ tumors, several groups have undertaken high throughput (HTP) analyses, including gene expression profiling assays[13,14] and proteomic-based approaches,[15,16] to discover selective ALK targets. Liquid chromatography–tandem mass spectrometry (LC-MS/MS) and HTP proteomics focusing on tyrosine phosphopeptides provide a fast and reliable method for large-scale analysis of cellular proteins differentially expressed in normal and tumor samples, and it is a powerful tool to identify selective signatures in kinase-driven hematologic and nonhematologic malignancies.[15,17-20]

Here we used 2 complementary proteomic-based approaches to dissect the ALK signaling. Taking advantage of shRNA and ALK kinase inhibitors, we compared the differential ALK tyrosine-phosphorylation profiling in different settings. We found that ALK activity is associated with a defined set of phosphorylated proteins regulating key cellular functions. Among novel ALK-associated proteins, we have shown that vasodilator-stimulated phosphoprotein (VASP) and ATIC are directly phosphorylated by ALK. The enzymatic activity of ATIC was enhanced after tyrosine phosphorylation via several oncogenes and phospho-ATIC was less efficiently inhibited by the methotrexate. These findings provide novel insights into ALK-mediated transformation and support the selection of tailored chemotherapeutic protocols.

Methods

Cell lines and reagents

Human ALCL cell lines TS (a subclone of Sup-M2), Sup-M2, JB-6, SU-DHL1, and Karpas-299 were previously described.[11-21] T-cell leukemic cell lines CCRF-CEM and Jurkat were obtained from ATCC (Manassas, VA); Mac-1 was kindly provided by Dr M. Kadin (Harvard University, Boston, MA). Cell lines were grown at 37°C in 5% CO_2 humidified air in RPMI 1640 medium (Lonza Verviers SPRL, Verviers, Belgium).

HEK-293T and HEK-293T-Rex Tet-on NPM-ALK cells[22] were grown at 37°C in 5% CO_2 humidified air in Iscove modified Dulbecco medium, supplemented with 10% fetal calf serum. For antiphosphotyrosine immunoprecipitation, HEK-293T-Rex Tet-on NPM-ALK cells were grown in nonadherent conditions on poly (2-hydroxyethylmethacrylate; Sigma-Aldrich, St Louis, MO)–coated plates, starved for 12 hours, and then induced with 1 μg/mL of tetracycline for 24 hours.

Self-inactivating retroviral particles for NPM-ALK and the kinase dead mutant NPM-ALK^{K210R} were produced as described previously.[11] Aliquots of virus, plus 8 μg/mL of polybrene, were used to infect exponentially growing cells (CCRF-CEM and Mac-1, 10^5/mL). Fresh medium was supplemented 24 hours after infection. The infectivity was determined after 72 hours of infection by fluorescence-activated cell sorting analysis of green fluorescent protein (GFP)–positive cells. GFP$^+$ cells were sorted by MoFlo High-Performance fluorescence-activated cell sorting (Dako North America, Carpinteria, CA) and expanded.

For the kinase inhibition experiments, NPM-ALK–positive and –negative cells were treated with 300 nM of CEP11988 or CEP14083[23] for 6 hours.

Phosphopeptide immunoprecipitation and LC-MS/MS mass spectrometry

Phosphopeptide immunoprecipitation from cell lines was performed as described previously[15] using the PhosphoScan Kit (P-Tyr-100) from Cell Signaling Technology (Danvers, MA; Document S1, available on the *Blood* website; see the Supplemental Materials link at the top of the online article).

All spectra and all sequence assignments obtained using Sequest (Thermo Scientific, Waltham, MA) were then imported into a relational database based on FileMaker Pro (FileMaker, Santa Clara, CA) and MySQL (Sun Microsystems, Santa Clara, CA), as described.[15] Comparison between large datasets was performed using a custom-made Perl script (www.perl.com), to find overlapping and/or recurrent sequences (see Document S1).

Anti-phosphotyrosine protein immunoprecipitation and LC/MS-MS analysis

Anti-phosphotyrosine immunoprecipitation on HEK-293T-Rex Tet-on cells (Invitrogen, Carlsbad, CA), transfected with a wild-type NPM-ALK or a kinase-dead mutant control NPM-ALK^{K210R}, and LC/MS-MS analyses were performed as previously described.[22] Protein identification via peptide MS/MS spectra was achieved using the Mascot software (http://matrixscience.com) for searching the National Center for Biotechnology Information nonredundant human protein database (released April 29, 2003; containing 37 490 protein sequences).

Stable isotope labeling of amino acid in cell culture analysis of shALK cells

Cells were grown in RPMI medium lacking arginine and lysine, supplemented with 10% dialyzed fetal bovine serum, penicillin/streptomycin, and L-lysine/HCl and L-arginine/HCl (Sigma-Aldrich) for light cultures or L-arginine/HCL (U-$^{13}C_6$, 98%) and L-lysine/2HCl (U-$^{13}C_6$, 98%; Cambridge Isotope Laboratories, Andover, MA) for heavy cultures as described.[24,25] Cells were grown to a density of approximately 10^6 cells/mL for a total of 10^8 cells per each cell culture type (2×10^8 cells total). After lysis, heavy and light cultures were combined and carried through the phosphopeptide immunoprecipitation protocol.

Protein immunoprecipitation and Western blotting

Immunoprecipitation and Western blot analysis were performed as described previously[26] (Document S1). The protein content of cell suspensions was assessed with the Lowry kit from Bio-Rad (Hercules, CA).

The following primary antibodies were used: mouse anti-ALK (1:4000, 4C5B8) and anti-STAT3 (5G7) from Zymed Laboratories (South San Francisco, CA); mouse anti–phospho-tyrosine (PY100; 1:2000), rabbit anti–phospho STAT3 (Tyr 705, 1:1000), rabbit antiphospho-ERK1/2 (Thr202/Thy204) (#9101 1:1000), rabbit anti–phospho-SHP2 (Tyr 542) (1:1000), rabbit anti–phospho-SHC (Tyr 317) (1:1000), rabbit anti–phospho-ALK (Tyr 1604) (1:1000), rabbit anti–SHC (1:1000), rabbit anti–p44/42 MAPK (1:1000), anti–VASP (1:1000), and rabbit anti–SHP2 (1:1000) from Cell Signaling Technology; mouse anti-actin (1:2000) from Millipore (Billerica, MA); mouse anti-ATIC (1:1000) from Abcam (Cambridge, United Kingdom) and agarose-conjugated 4G10 from Upstate Biotechnology (Charlottesville, VA).

Enzyme-kinase assay

ATIC enzyme and NPM-ALK kinase were immunoprecipitated from 2 mg of HEK-293T and HEK-293T NPM-ALK total cell lysate, respectively. The immunoprecipitated proteins were resuspended in kinase buffer (25 mM Tris-HCl, pH 7.5, 2 mM dithiothreitol (DTT), 0.1 mM Na_3VO_4, 10 mM $MgCl_2$, 5 mM b-glycerophosphate) and then combined at an equal ratio. The reaction was started by adding 0.2 mM adenosine triphosphate (ATP) to the mixture and incubating for 30 minutes at 37°C and then stopped by freezing the samples at −80°C.

Downloaded from http://ashpublications.net/blood/article-pdf/113/12/2776/1305103/zh801209002776.pdf by guest on 20 May 2024

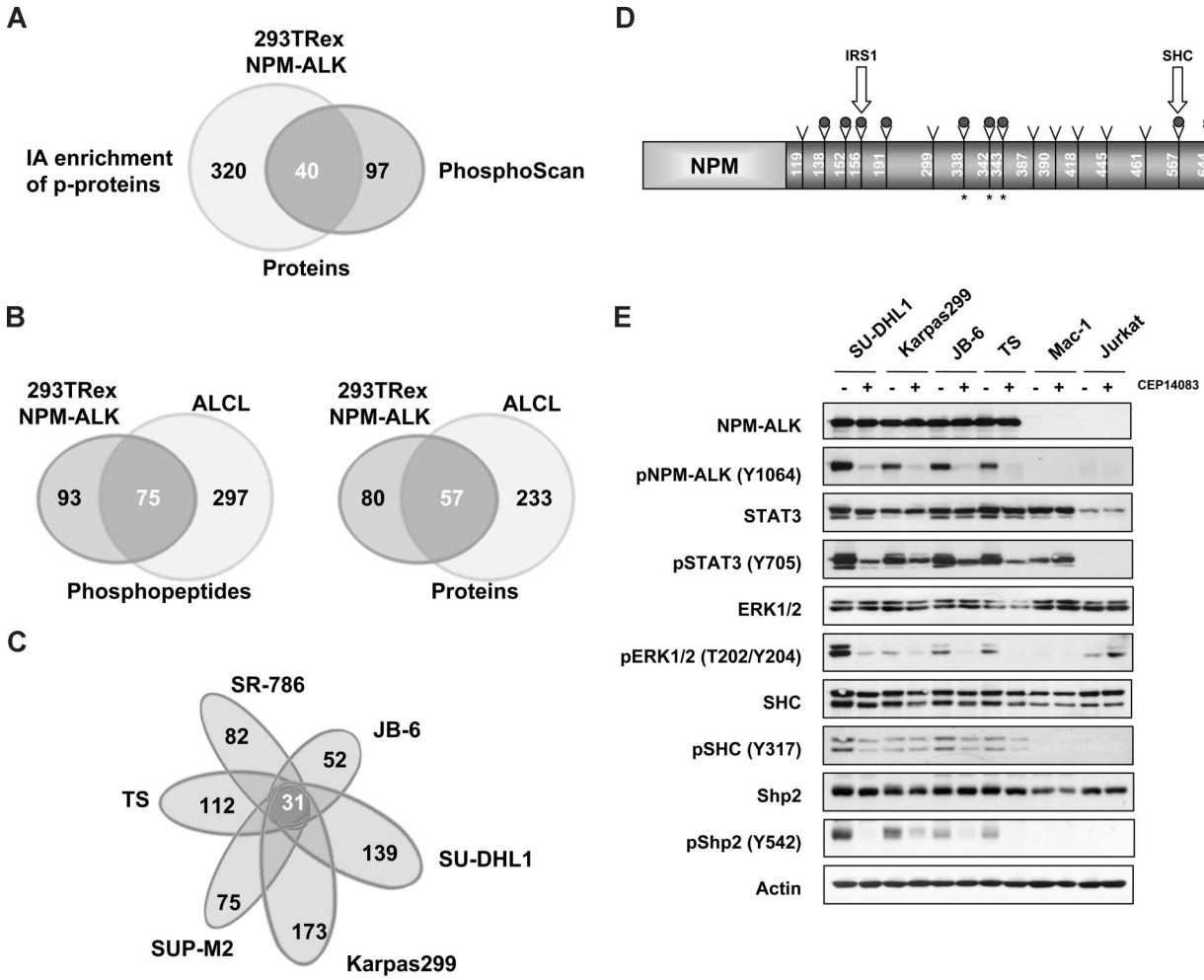

Figure 1. LC-MS/MS profiling of NPM-ALK$^+$ cells identifies a common set of Tyr-phosphorylated proteins. (A) Comparison of the datasets derived from the immunoaffinity (PhosphoScan) and conventional LC-MS/MS-based proteomic approaches (Table 1). (B) Immunoaffinity profiling of NPM-ALK$^+$ ALCL cell lines compared with NPM-ALK-positive HEK-293T-Rex cells. (C) Comparative PhosphoScan performed on 6 different ALCL cell lines. (D) Tyrosine phosphorylated sites on the NPM-ALK protein are represented with a gray dot (9 of these were identified in all ALK$^+$ cell lines); the star represents newly discovered sites. Tyrosine sites known to interact with IRS1, SHC, and PLC-g are indicated. (E) The phosphorylation status of selected proteins was assessed in ALCL cell lines after treatment with CEP14083 and detected by phospho-specific antibodies as indicated.

Where indicated, CEP14083 (300 nM) was added to the reaction mixture before adding ATP, then incubated for 30 minutes at 37°C. Methotrexate (MTX) was added at the indicated concentrations, and the reaction mixture was incubated again at 37°C for 2 hours.

Measurement of AICAR-FT/IMP-CHase activity

The synthesis of N^{10}-formyl-tetrahydrofolate from (6R, 6S)-5-formyltetrahydropteroil-L-glutamate was performed according to Uyeda and Rabinowitz.[27] The amount of N^{10}-formyl-tetrahydrofolate was assessed by measuring the absorbance at 298 nm ($\epsilon = 9.54\ cm^{-1}\cdot M^{-1}$). AICAR-FT activity was evaluated by coupling it with the reactions of serine-hydroxy-methyltransferase and methylene-tetrahydrofolate reductase[28]: 50 μg of total cellular lysates or immunoprecipitated proteins was resuspended in the following 1-mL reaction mix: 66 mM Tris (pH 7.4), 20 mM K_3PO_4, 5 mM DTT, 2 mM N^{10}-formyl-tetrahydrofolate, 1 mM AICAR. After 5 minutes, samples were incubated at 37°C in the presence of 1 mM L-serine, 0.2 μg serine-hydroxy-methyltransferase, and 0.2 μg of methylene-tetrahydrofolate reductase. Then (after 2 minutes), 0.05 mM nicotinamide adenine dinucleotide phosphate was added and the absorbance at 340 nm was measured for 10 minutes using a Lambda 3 spectrophotometer (PerkinElmer Life and Analytical Sciences, Waltham, MA). Preliminary experiments showed that, in these experimental conditions, the oxidation rate of nicotinamide adenine dinucleotide phosphate was linear throughout the observation time and stoichiometrically equivalent to the rate of AICAR disappearance by AICAR-FT (data not shown). Results were expressed as nmol $NADP^+$/minute per mg cell proteins.

The activities of IMP-CHase or AICAR-FT plus IMP-CHase were measured by a coupling assay with inosine 5′-monophosphate dehydrogenase[29]; 50 μg of total cellular lysates or immunoprecipitated proteins were incubated 30 minutes at 37°C in a reaction mix containing 66 mM Tris (pH 7.4), 5 mM DTT, 50 mM KCl (final volume, 1 mL). To detect the activity of IMP-Chase, 0.1 mM N-formylaminoimidazole-4-carboxamide ribonucleotide (F-AICAR), synthesized as previously described[30] and quantified by measuring the absorbance at 268 nm ($\epsilon = 10\ 900\ cm^{-1}\cdot M^{-1}$), was added. For the total activity of AICAR-FT plus IMP-CHase, samples were incubated with 2 mM N^{10}-formyl-tetrahydrofolate and 1 mM AICAR instead of F-AICAR. Then 0.1 μg inosine 5′-monophosphate dehydrogenase and 0.1 mM NAD^+ were added. The reduction rate of NAD^+, stoichiometrically equivalent to the rate of IMP synthesis under these experimental conditions (data not shown), was evaluated by measuring the absorbance at 340 nm. The reaction was linear throughout a 10-minute observation time and the results were expressed as nmol NADH/min/mg cell proteins.

Measurement of 6-phosphate dehydrogenase, 6-phosphogluconate dehydrogenase, lactic dehydrogenase, and ornithine decarboxilase activities

Enzymatic activity for glucose 6-phosphate dehydrogenase (G6PD), 6-phosphogluconate dehydrogenase (6PGD), and lactic dehydrogenase (LDH) was measured as previously described.[31] Ornithine decarboxilase activity was determined as the amount of $^{14}CO_2$ released from 0.5 μCi DL-[1-^{14}C]ornithine, as described.[32]

Downloaded from http://ashpublications.net/blood/article-pdf/113/12/2776/1305103/zh801209002776.pdf by guest on 20 May 2024

Table 1. Proteins identified in HEK 293T NPM-ALK cells by 2 complementary proteomic approaches

Gene symbol	NCBI access no.	Protein	No. of peptides*	Sequence coverage,* %
Kinases and phosphatases				
ALK	NP_004295	Anaplastic lymphoma kinase Ki-1	30	38
GSK3A	NP_063937	Glycogen synthase kinase 3 α	1	2
PFKP	NP_002618	Phosphofructokinase, platelet	3	3
PKM2	NP_872270	Pyruvate kinase 3 isoform 2	8	20
PTPN11	NP_002825	Shp2	4	6
Metabolism				
ACLY	NP_001087	ATP citrate lyase	6	6
CUL2	NP_003582	Cullin 2	5	9
DDX3X	NP_004651	DEAD/H box-3	5	7
DNAJC7	NP_003306	DnaJ (Hsp40) homolog	7	13
ENO1	NP_001419	Enolase 1	48	57
HNRPA1	NP_112420	Heterogeneous nuclear ribonucleoprotein A1	5	22
HNRPA2B1	NP_112533	Heterogeneous nuclear ribonucleoprotein A2/B1	11	30
HNRPF	NP_004957	Heterogeneous nuclear ribonucleoprotein F	3	8
HNRPH1	NP_005511	Heterogeneous nuclear ribonucleoprotein H1	2	3
HNRPR	NP_005817	Heterogeneous nuclear ribonucleoprotein R	2	3
HNRPU	NP_004492	Heterogeneous nuclear ribonucleoprotein U	11	12
SFPQ	NP_005057	Splicing factor proline/glutamine rich	5	5
TARS	NP_689508	Threonyl-tRNA synthetase	3	4
ZNF598	NP_835461	Zinc finger protein 598		
Adaptor proteins				
HGS	NP_004703	Hepatocyte growth factor-regulated tyrosine kinase substrate	3	4
HSP90AB1	NP_031381	Heat shock 90-kDa protein 1, β	25	25
HSPA1B	NP_005337	Heat shock 70-kDa protein 1B	16	28
HSPA2	NP_068814	Heat shock 70-kDa protein 2	1	1
HSPA4	NP_002145	Heat shock 70-kDa protein 4	1	1
HSPA8	NP_006588	Heat shock 70-kDa protein 8	1	3
IRS4	NP_003595	Insulin receptor substrate 4	48	27
RPLP0	NP_444505	Ribosomal protein P0	3	10
SHC	NP_003020	SHC	2	2
TRAP1	NP_057376	Tumor necrosis factor type 1 receptor-associated protein	1	2
Signal transduction				
ARHGEF2	NP_004714	rho/rac guanine nucleotide exchange factor 2	1	1
CNOT1	NP_057368	KIAA1007 protein; CCR4-NOT transcription complex, subunit 1	1	1
LMO7	NP_005349	LIM domain only 7	1	1
STAT3	NP_644805	Signal transducer and activator of transcription 3	2	2
YWHAG	NP_036611	14-3–3 γ	7	24
Cytoskeleton				
ACTB	NP_001092	β actin	8	20
BICD2	NP_056065	Bicaudal D homolog 2	7	11
VIM	NP_003371	Vimentin	18	38
Unknown function				
FHL1	NP_001440	Four and a half LIM domains 1	2	6
NCAPH	NP_056156	Barren	7	13
UBAP2L	NP_055662	NICE-4 protein	4	6

*Number of peptides and sequence coverage refer to IA enrichment method only.

Results

LC-MS/MS identifies a set of phosphotyrosine peptides in NPM-ALK$^+$ cells

To determine a global profile of tyrosine (Tyr)–phosphorylated proteins in NPM-ALK cells, we used 2 different LC-MS/MS-based proteomic approaches. Both methods implied immunoaffinity precipitation of Tyr-phosphorylated proteins by specific anti–phosphotyrosine antibodies, but whereas the first approach required the excision of bands of interest from sodium dodecyl sulfate–polyacrylamide gel electrophoresis (15-20 bands differentially expressed, compared with control), the second approach allowed a more global mapping of Tyr-phosphorylated peptides. We have first assessed the feasibility of both strategies using a tetracycline-inducible NPM-ALK HEK-293T-Rex cell line (Figure 1A). A list of 40 common proteins detected by both approaches is provided in Table 1. These studies confirmed several known interactors of NPM-ALK (STAT3, SHC, and PTPN11)[21,26,33] and discovered novel Tyr-phosphorylated proteins. The immunoaffinity profiling of phosphopeptides (PhosphoScan)[15] identified a total of 167 peptides (corresponding to 137 phosphorylated proteins), granting a better specificity compared with conventional approaches (Table S1). This technique excludes all proteins that are not phosphorylated but bind specifically to a phosphorylated peptide and identifies multiple Tyr-phosphorylated peptides corresponding to the same protein, providing a higher degree of confidence.

Given that the HEK-293T–inducible system uses a highly controlled but ectopic NPM-ALK expression in a nonlymphoid cells, we applied the PhosphoScan technology (Cell Signaling

Downloaded from http://ashpublications.net/blood/article-pdf/113/12/2776/1305103/zh801209002776.pdf by guest on 20 May 2024

Table 2. Tyrosine phosphorylated peptides identified by PhosphoScan in 6 ALK$^+$ ALCL cell lines (cutoff level, 67%) versus the ALK$^-$ cell line Mac-1

Gene symbol	pTyr site	Peptide	Karpas299	SU-DHL1	JB-6	TS	SR-786	SUP-M2	Mac-1
Kinases									
ALK	1078*	HQELQAMQMELQSPEyK	●	●	●	●	●	●	
ALK	1092*	TSTIMTDyNPNYCFAGK	●	●	●	●	●	●	
ALK	1096*	TSTIMTDYNPNyCFAGK	●	●	●	●	●	●	
ALK	1131*	GLGHGAFGEVyEGQVSGMPNDPSPLQVAVK	●			●	●	●	
ALK	1278*	DIyRASYYR	●	●	●	●	●	●	
ALK	1282*	DIyRASyYR	●	●	●	●	●	●	
ALK	1283*	DIyRASyyR	●	●	●	●	●	●	
ALK	1507*	NKPTSLWNPTyGSWFTEKPTK	●	●	●	●	●	●	
ALK	1584*	HFPCGNVNyGYQQQGLPLEAATAPGAGHyEDTILK	●	●		●		●	
ALK	1586*	HFPCGNVNYGyQQQGLPLEAATAPGAGHyEDTILK	●	●	●	●	●	●	
ALK	1604*	HFPCGNVNYGyQQQGLPLEAATAPGAGHyEDTILK	●	●	●	●	●	●	
CDC2	15	IEKIGEGTyGVVYK		●	●	●	●	●	●
CDK3	15	VEKIGEGTyGVVYK	●	●	●	●	●	●	●
DYRK1A	321	IYQyIQSR	●	●	●	●	●	●	●
GSK3B	279	GEPNVSyICSR	●	●	●	●	●	●	●
HIPK1	352	AVCSTyLQSR	●	●		●	●	●	●
MAPK1	187	VADPDHDHTGFLTEyVATR	●	●	●	●	●		●
PGK1	195	ELNyFAK, KELNyFAK	●	●	●	●		●	
PIP5K2B	93	FKEyCPMVFR	●			●	●	●	
PRPF4B	849	LCDFGSASHVADNDITPyLVSR	●	●	●	●	●	●	●
Metabolism									
ACLY	682	TTDGVyEGVAIGGDRYPGSTFMDHVLR	●	●	●	●	●	●	
ATIC	104	VVACNLyPFVK	●	●	●	●	●	●	
DCP1B	110	LSIyGIWFYDKEECQR	●	●			●	●	
EIF3S7	318	NLAMEATyINHNFSQQCLR	●		●	●		●	
EIF3S9	525	NGDyLCVK	●	●		●	●	●	
ELP3	202	NLHDALSGHTSNNIyEAVK	●	●		●	●	●	
ENO1	43	AAVPSGASTGIyEALELR	●	●	●	●	●	●	●
ENO1	286	SFIKDyPVVSIEDPFDQDDWGAWQK	●	●			●	●	
HIST1H4I	51	ISGLIyEETR	●	●			●	●	
HNRPF	306	ATENDIyNFFSPLNPVR	●	●			●	●	
HSPCB	483	SIyYITGESKEQVANSAFVER	●	●	●	●	●	●	
LDHA	238	QVVESAyEVIK	●	●	●	●	●	●	●
LDHB	239	MVVESAyEVIK	●	●	●	●	●	●	●
MDH2	56	LTLyDIAHTPGVAADLSHIETK		●	●	●	●		
NIT2	145	TLSPGDSFSTFDTPyCR	●	●	●	●	●	●	
NYREN18	126	SKIAETFGLQENyIK	●		●	●	●		
PABPC1	54	SLGyAYVNFQQPADAER	●	●	●	●	●	●	
PBEF1	188	YLLETSGNLDGLEyKLHDFGYR	●	●	●	●	●		
PKM2	104	TATESFASDPILyRPVAVALDTKGPEIR	●	●	●	●	●	●	●
PRIM2A	381	IILSNPPSQGDyHGCPFR	●	●	●	●	●		
PSMA2	23	LVQIEyALAAVAGGAPSVGIK	●	●	●	●	●		
PSMA2	97	KLAQQYyLVYQEPIPTAQLVQR	●	●	●	●	●		
PSMB4	102	VNNSTMLGASGDyADFQYLK	●	●		●	●	●	
RNPS1	205	GyAYVEFENPDEAEK	●	●			●	●	
RPL18A	63	SSGEIVyCGQVFEK	●	●	●	●	●	●	
RPL31	103	NEDEDSPNKLyTLVTYVPVTTFK	●	●	●	●	●	●	
RPL7	139	IVEPyIAWGYPNLK	●		●	●	●	●	
RPLP0	24	IIQLLDDyPKCFIVGADNVGSK	●	●	●	●	●	●	●
RPS13	37	LTSDDVKEQIyK	●	●		●		●	
TXNRD1	11	SyDYDLIIIGGGSGGLAAAK	●	●	●	●			
TXNRD1	13	SYDyDLIIIGGGSGGLAAAK	●	●	●	●	●	●	
WDR54	33	NLTyFGVVHGPSAQLLSAAPEGVPLAQR	●	●			●	●	
G-proteins									
GDI2	203	TDDYLDQPCyETINR	●	●		●		●	●
RASA1	615	HFTNPyCNIYLNSVQVAK	●	●	●	●	●	●	
Adaptor proteins									
GRLF1	1105	NEEENIySVPHDSTQGK		●		●	●		
HSPA4	336	LKKEDIyAVEIVGGATR	●	●		●	●	●	
HSPD1	227	GYISPyFINTSK	●	●			●	●	

*The indicated ALK pTyr sites refer to the full lenght ALK receptor, and they correspond to NPM-ALK pTyr sites 138, 152, 156, 191, 338, 342, 343, 567, 644, 646, and 664, respectively

Downloaded from http://ashpublications.net/blood/article-pdf/113/12/2776/1305103/zh801209002776.pdf by guest on 20 May 2024

Table 2. Tyrosine phosphorylated peptides identified by PhosphoScan in 6 ALK$^+$ ALCL cell lines (cutoff level, 67%) versus the ALK$^-$ cell line Mac-1 (continued)

Gene symbol	pTyr site	Peptide	Karpas299	SU-DHL1	JB-6	TS	SR-786	SUP-M2	Mac-1
IRS1	46	AASEAGGPARLEyYENEKK		●		●	●		
SHC1	427	ELFDDPSyVNVQNLDK	●	●	●	●	●	●	●
TRAP1	498	NIyYLCAPNR	●	●	●	●	●	●	
Transcription factors									
EEF1A1	141	EHALLAyTLGVK	●	●	●	●	●		●
STAT3	704	YCRPESQEHPEADPGAAPyLK	●	●	●	●	●	●	●
STAT3	705	YCRPESQEHPEADPGSAAPyLK	●	●	●	●	●	●	●
Cytoskeleton									
ACTB	218	DIKEKLCyVALDFEQEMATAASSSSLEK	●	●		●	●		
DNCH1	3379	NYMSNPSYNyEIVNR	●	●	●		●	●	
STOML2	124	ASYGVEDPEyAVTQLAQTTMR	●	●		●	●		
VASP	38	VQIyHNPTANSFR	●	●	●	●	●		
VIM	116	TNEKVELQELNDRFANyIDKVR, FANyIDKVR	●			●	●	●	
WDR1	238	AHDGGIyAISWSPDSTHLLSASGDKTSK	●	●		●	●	●	

*The indicated ALK pTyr sites refer to the full-length ALK receptor, and they correspond to NPM-ALK pTyr sites 138, 152, 156, 191, 338, 342, 343, 567, 644, 646, and 664, respectively

Technology) to a panel of NPM-ALK–positive ALCL lines, a model that better reproduces the ALK lymphoproliferative processes. This analysis revealed a total of 372 Tyr-phosphorylated peptides within 290 proteins (Figure 1B), which included approximately half of the peptides previously identified in NPM-ALK HEK-293T cells. A further analysis, performed to find the proteins shared by all cell lines and applying both techniques (data not shown), led to the discovery of a small cluster of 26 Tyr-phosphorylated proteins (Table S2), which were also largely represented in previous analyses. We then compared the data obtained from the phospho-tyrosine immunoprecipitation of 6 ALK$^+$ ALCL lines and found a panel of 372 peptides (within 290 different proteins), 31 of which were shared by all 6 ALCL cell lines (Figure 1C).

Of these 31 Tyr-phosphorylated peptides, 12 were also shared by the ALK$^-$ control T cell lymphoblastoid line Mac-1 (CD30/STAT3/STAT5-positive). These phosphopeptides belonged to proteins with kinase activity (GSK3B (Y279), CDK3 (Y15), DYRK1A (Y321), PRPF4B (Y849]) or metabolic enzymes (ENO-1 [Y43], LDH-A [Y238], LDH-B [Y239], PKM [Y104]) frequently found in proliferating cells. Notably, some well-documented ALK interactors, such as SHC-1 (Y427) and STAT3 (iso1 Y704, and iso2 Y705), were also found. Similar findings were obtained by comparison of ALK$^+$ cell lines to other 2 ALK$^-$ lymphoid cell lines (CCRF-CEM and Jurkat, data not shown).

Nineteen peptides were exclusively found in ALK$^+$ cells, and 9 belonged to the ALK protein itself. Noteworthy, 4 of these were novel ALK phosphorylation sites (Figure 1D). The remaining 10 peptides identified proteins linked to cell metabolism, including ATIC (Y104) and ATP-citrate lyase (ACLY, Y682), G-proteins (GTPase-activating protein RasA1, Y615), and ribosomal proteins (RPs) L31 (Y103) and L18a (Y63). Using a lower cutoff level (peptides identified in $>$ 4 of 6 cell lines), we could define a larger protein set with several novel entities (Table 2); among them, ribosomal (L7 [Y139], S13 [Y37], and P0 [Y24]) and structural proteins, including VASP (Y38), a cytoskeletal-regulating protein recently identified as part of BCR-ABL phospho-tyrosine signature.[17]

ALK inhibition defines a common phospho-tyrosine signature

To identify phosphorylated proteins playing a pathogenic role in NPM-ALK-mediated transformation, we analyzed the Tyr-phosphorylation signature of ALK$^+$ ALCL lines after abrogating the expression or the activity of NPM-ALK by RNA interference (RNAi)[11] or by a small molecule ALK inhibitor,[23] respectively. Using an inducible shRNA and quantitative proteomic approach, we demonstrated that a total of 101 peptides were no longer phosphorylated after ALK silencing, whereas 24 became phosphorylated and 35 were apparently unaffected by ALK RNAi (Table S3).

To exclude off-target effects by RNAi, ALCL cells were treated with a small-molecule ALK inhibitor (CEP14083) or by a control compound (CEP11988).[23] These studies revealed a total of 138 phosphopeptides lost after ALK inhibition, whereas 109 new peptides became phosphorylated and 226 were unchanged after ALK inhibition (Table S4), with a good overlap between the RNAi and ALK inhibitor datasets. Nevertheless, small or no variations of well-known ALK-related Tyr-phosphorylated proteins were seen by the single approach or the combined methods (ie, STAT3). Thus, we used a Stable Isotope Labeling of Amino acid in Cell culture approach on TS cells after induction of a specific ALK shRNA. The PhosphoScan technology allowed the identification of variations in the phosphorylation levels of many proteins, including known NPM-ALK downstream targets and novel proteins, undetectable using previous analyses (Table 3). For instance, a significant down-modulation of p-STAT3 signal (13-fold inhibition) was observed after ALK silencing. Moreover, Western blot validation confirmed the abrogation of NPM-ALK–dependent phosphorylation of several downstream targets (Figure 1E). A combined approach may identify a common set of tyrosine-phosphorylated proteins whose status correlates more precisely to ALK activity.

NPM-ALK induces ATIC and VASP phosphorylation

To validate new ALK interactors, we selected 2 biologically relevant proteins: ATIC and VASP. ATIC is an enzyme involved in purine biosynthesis and VASP is a protein regulating actin polymerization and cytoskeletal reorganization.[3,34] The MS/MS spectra of both phosphopeptides displayed an Xcorr value larger than 2.3 and a well-represented proline peak, suggesting a correct assignment[35] (Figure 2A,B). Phosphorylated ATIC and VASP were confirmed by immunoprecipitation and Western blot in all NPM-ALK–positive lines. Notably, ATIC Tyr-phosphorylation was also detectable in control lines (CEM and Jurkat), suggesting that ATIC might be a

Downloaded from http://ashpublications.net/blood/article-pdf/113/12/2776/1305103/zh801209002776.pdf by guest on 20 May 2024

Table 3. Tyrosine phosphorylated peptides that changed their phosphorylation status while ALK was inhibited by shRNA or a pharmacologic inhibitor

Gene symbol	Peptide	PTyr site	Protein	*Average H:L	NCBI access no.	shALK	ALK inhibitor
Peptides that decrease when ALK is reduced							
Kinases							
ALK	R.TSTIMTDYNPNY*CFAGK	1096	Anaplastic lymphoma kinase	1:6.20	NP_004295	1	1
ALK	R.NKPTSLWNPTY*GSWFTEKPTK	1507	Anaplastic lymphoma kinase	1:3.72	NP_004295	2	1
CDC2	K.IEKIGEGTY*GVVYK	15	Cell division cycle 2 protein	1:2.7	NP_203698	2	1
CDK2	K.VEKIGEGTY*GVVYK	15	Cyclin dependent kinase 2	>1:6	NP_001789	2	1
ERK1/MAPK3	R.IADPEHDHTGFLTEY*VATR	187	Mitogen-activated protein kinase 3	1:2.07	NP_002737	Not found	2
p38/MAPK14	R.HTDDEMTGY*VATR	182	Mitogen-activated protein kinase 14	1:3.22	NP_620581	2	1
Adaptors							
HGS	R.VCEPCY*EQLNR	216	HGF regulated tyrosine kinase substrate	>1:4	NP_004703	Not found	1
PAG	K.SGQSLTVPESTY*TSIQGDPQR	341	Phosphoprotein associated with glycosphingo	1.47:1	NP_060910	Not found	3
PARD3	R.DVTIGGSAPIY*VK	489	par-3 partitioning defective 3 homolog	>1:4	NP_062565	Not found	2
Cytoskeletal proteins							
ACTB	R.KDLY*ANTVLSGGTTMYPGIADR.M	294	Actin, β	1:5.71	NP_001092	1	Not found
ACTB	K.EKLCY*VALDFEQEMATAASSSSLEK.S	218	Actin, β	>1:3	NP_001092	1	1
CORO1C	R.YFEITDESPY*VHYLNTFSSK.E	301	Coronin, actin binding protein, 1C	1:2.47	NP_055140	3	1
VASP	R.VQIY*HNPTANSFR.V	39	Vasodilator-stimulated phosphoprotein	>1:9	NP_003361	1	1
VIM	R.FANY*IDKVR.F	117	Vimentin	>1:6	NP_003371	2	1
Chaperones							
HSP90AB1	K.SIY*YITGESK.E	484	Heat shock protein 90kDa α	1:2.74	NP_031381	4	1
HSPA2	R.TTPSY*VAFTDTER.L	43	Heat shock 70kDa protein 2	>1:2	NP_068814	Not found	1
HSPA4	K.LKKEDIY*AVEIVGGATR.I	336	Heat shock 70kDa protein 4	1:2.66	NP_002145	2	1
TRAP1	R.NIY*YLCAPNR.H	498	TNF receptor-associated protein 1	1:2.9	NP_057376	1	1
Cytokines							
PBEF	K.YLLETSGNLDGLEY*KLHDFGYR.G	188	Pre-B-cell colony enhancing factor 1	1:2.04	NP_005737	1	1
Energy metabolism							
RASA1	K.HFTNPY*CNIYLNSVQVAK.T	615	RAS p21 protein activator 1	1:3.25	NP_072179		
Metabolic enzymes							
ACLY	R.TTDGVY*EGVAIGGDRYPGSTFMDHVLR.Y	682	ATP cytrate lyase	1:4.27	NP_001087	1	1
ACP1	K.QLIIEDPYYGNDSDFETVY*QQCVR.C	143	Acidic phosphatase 1	1:5.2	NP_004291	2	1
ATIC	VVACNLyPFVK	104	AICAR formyltransferase/IMP Chase	1:3.70	NP_004035	1	1
ELP3	R.NLHDALSGHTSNNIY*EAVK.Y	202	Elongation protein 3	1:5.57	NP_060561	2	1
ENO1	K.SFIKDY*PVVSIEDPFDQDDWGAWQK.F	287	Enolase 1	1:2.91	NP_001419	1	1
GBE1	R.EGDNVNY*DWIHWDPEHSYEFK.H	173	Glucan (1,4-α-), branching enzyme 1	1:1.86	NP_000149	3	1
LDHA	K.QVVESAY*EVIK.L	239	Lactate dehydrogenase A	1:3.03	NP_005557	2	1
LDHB	K.MVVESAY*EVIK.L	240	Lactate dehydrogenase B	1:4.00	NP_002291	1	1
NIT2	K.TLSPGDSFSTFDTPY*CR.V	145	Nitrilase family, member 2	1:4.14	NP_064587	1	1
NUDT5	R.TLHY*ECIVLVK.Q	74	Nudix-type motif 5	1:10.3	NP_054861	2	1
PFKFB3	R.ISCY*EASYQPLDPDKCDR.D	194	6-Phosphofructo-2-kinase	>1:8	NP_004557	Not found	3
PKM2	R.TATESFASDPILY*RPVAVALDTKGPEIR.T	105	Pyruvate kinase 3	1:4.56	NP_002645	1	1
SUCLA2	K.SPDEAY*AIAK.K	84	succinate-CoA ligase, ADP-forming, β sub	>1:2.64	NP_003841	Not found	1

Average H:L indicates SILAC quantification performed on samples treated with ALK shRNA.
1Phosphopeptides that are present both in CEP11988 and CEP14083, in shALK$^-$ and shALK$^+$.
2Phosphopeptides that are present in CEP11988 and in shALK$^-$, but not in CEP14083 and shALK$^+$.
3Phosphopeptides that are present in CEP14083 and shALK$^+$, but not in CEP11988 and in shALK$^-$.
4Phosphopeptides detected twice with ambiguous results.

Downloaded from http://ashpublications.net/blood/article-pdf/113/12/2776/1305103/zh801209002776.pdf by guest on 20 May 2024

Table 3. Tyrosine phosphorylated peptides that changed their phosphorylation status while ALK was inhibited by shRNA or a pharmacologic inhibitor (continued)

Gene symbol	Peptide	PTyr site	Protein	*Average H:L	NCBI access no.	shALK	ALK inhibitor
Metabolism of nucleic acids							
HIST1H4I	R.ISGLIY*EETR.G	52	H4 histone family	1:2.45	NP_068803	4	1
HNRPF	K.ATENDIY*NFFSPLNPVR.V	306	Heterogeneous nuclear ribonucleoprotein F	>1:3	NP_004957	Not found	2
MKI67IP	R.TGNSKGY*AFVEFESEDVAK.I	88	FHA domain interacting nucleolar phosphopro	1:2.8	NP_115766	Not found	1
PABP 1	R.SLGY*AYVNFQQPADAER.A	56	Poly A binding protein, cytoplasmic 4	>1:8	NP_003810	2	1
POLR2A	R.LTHVY*DLCK.G	145	DNA directed RNA pol. II polyp. A	1:3.58	NP_000928	2	1
RNPS1	K.GY*AYVEFENPDEAEK.A	205	RNA binding prot S1, serine-rich domain	>1:4	NP_542161	4	1
SFPQ	R.FAQHGTFEY*EYSQR.W	488	Splicing factor proline/glutamine rich (polypyri	1:3.63	NP_005057	2	3
SYNCRIP	K.LKDY*AFIHFDERDGAVK.A	373	Synaptotagmin binding, cytoplasmic RNA inte	1:3.88	NP_006363	Not found	2
Regulation of translation							
PHF19	K.LTEGQY*VLCR.W	45	PHD finger protein 19	1:3.5	NP_082992	Not found	2
PHB2	R.IPWFQY*PIIYDIR.A	77	Prohibitin 2	1:3.43	NP_009204	Not found	1
PHB2	R.LGLDY*EER.V	128	Prohibitin 2	1:1.93	NP_009204	Not found	3
EEF1A1	K.STTTGHLIY*K.C	29	Eukaryotic elongation factor 1 α 1	>1:3	NP_001393	Not found	3
EIF3S2	K.SYSSGGEDGY*VR.I	308	Eukaryotic translation initiation factor 3	>1:13	NP_003748	2	1
EIF3S9	K.NGDY*LCVK.V	525	Eukaryotic translation initiation factor 3, subun	1:3.75	NP_003742	2	1
EIF3S7	R.NLAMEATY*INHNFSQQCLR.M	318	Eukaryotic translation initiation factor 3,subun	1:2.68	NP_003744	4	1
KNTC2	R.AQVY*VPLKELLNETEEEINK.A	458	Kinetochore associated 2	>1:5	NP_006092	Not found	1
Ribosomal proteins							
RPL18A	K.SSGEIVY*CGQVFEK.S	63	Ribosomal protein L18a	1:3.16	NP_000971	1	1
RPL31	R.NEDEDSPNKLY*TLVTYVPVTTFK.N	103	Ribosomal protein L31	1:2.87	NP_000984	1	1
RPL7	R.IVEPY*IAWGYPNLK.S	139	Ribosomal protein L7	1:2.10	NP_000962	2	1
RPL8	R.ASGNY*ATVISHNPETK.K	133	Ribosomal protein L8	1:3.15	NP_000964	1	1
RPLP0	K.IIQLLDDY*PK.C	24	Ribosomal protein P0	1:5.23	NP_000993	4	1
RPS10	R.IAIY*ELLFK.E	12	Ribosomal protein S10	1:2.52	NP_001005	Not found	1
RPS13	K.LTSDDVKEQIY*K.L	38	Ribosomal protein S13	1:1.8	NP_001008	Not found	1
Transcription factors							
DCP1A	R.SASPY*HGFTIVNR.L	64	DCP1 decapping enzyme homolog A	1:2.24	NP_060873	Not found	1
STAT3 iso1	K.YCRPESQEHPEADPGSAAPY*LK.T	705	Signal transducer and activator of transcriptio	1:13.23	NP_644805	1	1
STAT3 iso2	K.YCRPESQEHPEADPGAAPY*LK.T	704	Signal transducer and activator of transcriptio	1:13.57	NP_003141	4	1
Ubiquitin-proteasome system							
PSMA2	K.LVQIEY*ALAAVAGGAPSVGIK.A	98	Proteasome subunit α type 2	1:4.37	NP_002778	2	1
PSMA2	R.KLAQQYY*LVYQEPIPTAQLVQR.V	24	Proteasome subunit α type 2	1:3.18	NP_002778	2	1
Others							
ANXA2	K.SLY*YYIQQDTK.G	316	Annexin A2	1:1.91	NP_004030	2	1
GSDMDC1	R.SRGDNVY*VVTEVLQTQK.E	71	Gasdermin domain containing 1	1:3.27	NP_079012	Not found	1
FAM62B	R.NLIAFSEDGSDPY*VR.M	796	Family with sequence similarity 62 member B	>1:3	NP_065779	2	3
WDR1	K.AHDGGIY*AISWSPDSTHLLSASGDK.T	98	WD repeat-containing protein 1	1:3.58	NP_005103	2	1

Average H:L indicates SILAC quantification performed on samples treated with ALK shRNA.
1Phosphopeptides that are present both in CEP11988 and CEP14083, in shALK$^-$ and shALK$^+$.
2Phosphopeptides that are present in CEP11988 and in shALK$^-$, but not in CEP14083 and shALK$^+$.
3Phosphopeptides that are present in CEP14083 and shALK$^+$, but not in CEP11988 and in shALK$^-$.
4Phosphopeptides detected twice with ambiguous results.

Downloaded from http://ashpublications.net/blood/article-pdf/113/12/2776/1305103/zh801209002776.pdf by guest on 20 May 2024

Table 3. Tyrosine phosphorylated peptides that changed their phosphorylation status while ALK was inhibited by shRNA or a pharmacologic inhibitor (continued)

Gene symbol	Peptide	PTyr site	Protein	*Average H:L	NCBI access no.	shALK	ALK inhibitor
Peptides with no significant change							
Kinases							
DYRK1A	R.KVYNDGYDDDNY*DYIVK.N	145	Dual-specificity tyr. phosphorylation regulated	1:1.15	NP_001387	2	1
DYRK1A	R.IYQY*IQSR.F	321	Dual-specificity tyr. phosphorylation regulated	1:1.36	NP_001387	1	1
GSK3	R.GEPNVSY*ICSR.Y	216	Glycogen synthase kinase 3 α	1:1.15	NP_063937	1	1
HIPK1	K.AVCSTY*LQSR.Y	352	Homeodomain interacting protein kinase 1	1:1.15	NP_689909	2	1
HIPK3	K.TVCSTY*LQSR.Y	359	Homeodomain interacting protein kinase 3	1:0.99	NP_005725	3	1
PRPF4B	K.LCDFGSASHVADNDITPY*LVSR.F	849	Serine/threonine-protein kinase PRP4K	1:1.02	NP_003904	1	1
SRC	R.LIEDNEY*TAR.Q	419 (416)	v-src sarcoma viral Oncogene homolog	1:1.10	NP_005408	Not found	Not found
Adaptors							
SHC	R.ELFDDPSY*VNVQNLDK.A	318	SHC 1	1:1.44	NP_003020	1	1
Chaperones							
HSPD1	R.GYISPY*FINTSK.G	227	Heat shock 60 kDa protein 1 (chaperonin)	1:1.35	NP_955472	Not found	1
HSP90AA1	K.HIY*YITGETK.D	492	Heat shock 90 kDa protein	1:1.18	NP_005339	Not found	1
Cytokines							
PBEF	K.VY*SYFECR.E	34	Pre-B-cell colony enhancing factor 1	1:1.02	NP_005737	2	1
Energy metabolism							
GDI2	R.TDDYLDQPCY*ETINR.I	203	GDP dissociation inhibitor 2	1:1.46	NP_001485	2	1
RAN	K.SNY*NFEKPFLWLAR.K	155	ras-related nuclear protein	1:1.12	NP_006316	Not found	1
WRNIP1	R.MLEGGEDPLY*VAR.R	534	Werner helicase interacting protein 1	1:1.20	NP_064520	2	1

Average H:L indicates SILAC quantification performed on samples treated with ALK shRNA.
1Phosphopeptides that are present both in CEP11988 and CEP14083, in shALK$^-$ and shALK$^+$.
2Phosphopeptides that are present in CEP11988 and in shALK$^-$, but not in CEP14083 and shALK$^+$.
3Phosphopeptides that are present in CEP14083 and shALK$^+$, but not in CEP11988 and in shALK$^-$.
4Phosphopeptides detected twice with ambiguous results.

Downloaded from http://ashpublications.net/blood/article-pdf/113/12/2776/1305103/zh801209002776.pdf by guest on 20 May 2024

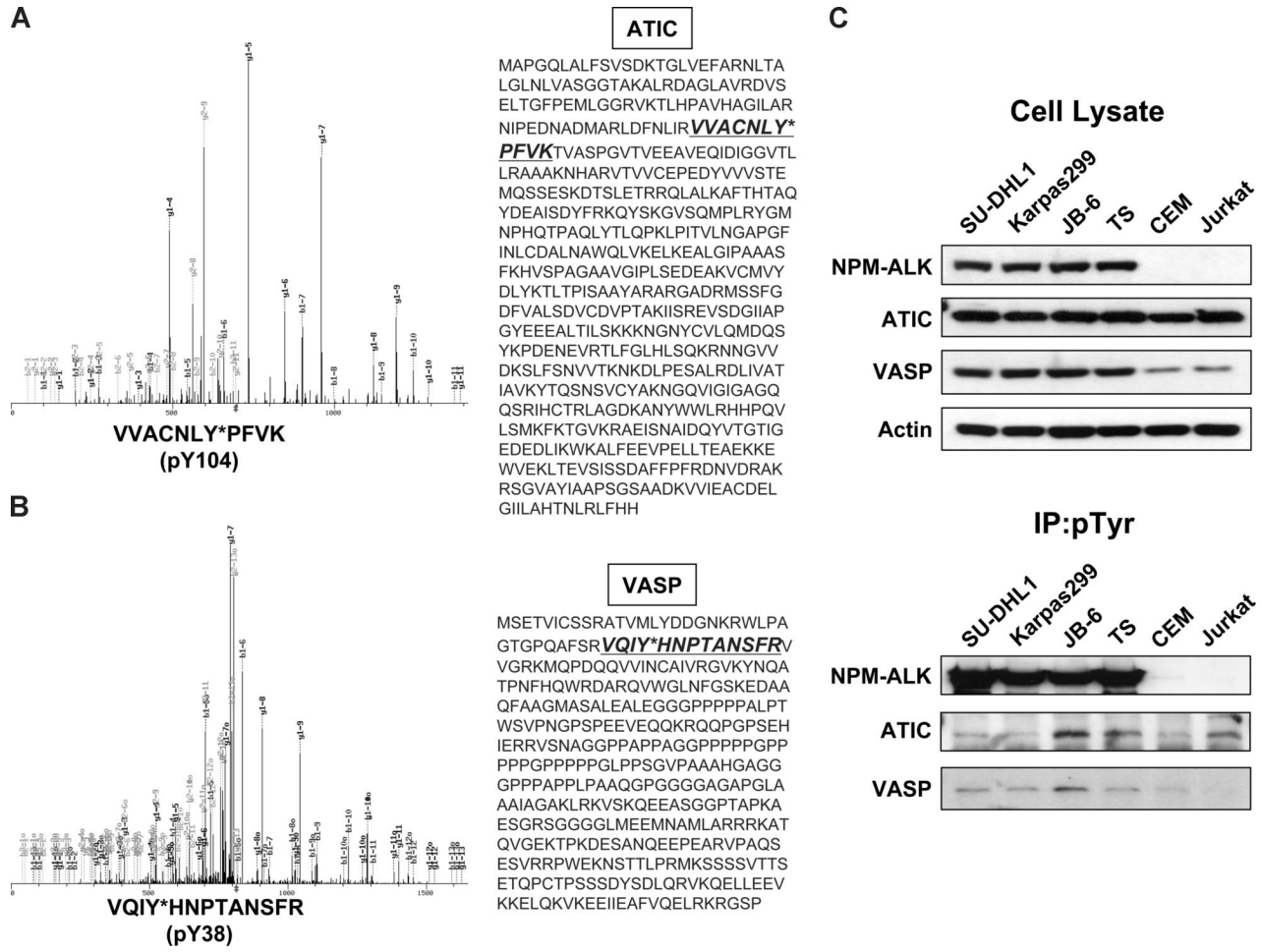

Figure 2. Tyrosine phosphopeptides are identified in ALK$^+$ ALCL cells. (A) MS/MS spectrum of tyrosine-phosphorylated peptide VVACNLYPFVK, assigned to the protein ATIC (percentage coverage, 1.8% of total sequence). (B) MS/MS spectrum of tyrosine-phosphorylated peptide VQIYHNPTANSFR, assigned to the protein VASP (percentage coverage, 3.4% of total sequence). (C) Total protein expressions (top panel) and phosphorylation status (bottom panel) as assayed by Western blot with the indicated antibodies.

substrate of other kinases (Figure 2C). In a subsequent survey of 243 cell lines, we found that p-ATIC (Tyr 104) was detectable in all ALK$^+$ ALCL, and in 1 of 3 non–small cell lung cancer lines carrying p-ALK. Among ALK$^-$ nonlymphoid samples, p-ATIC was documented in 5 of 237 lines expressing activated kinases (ABL, EGFR, and PDGFR) and 7 of 148 tumor samples, some of which displayed detectable p-Met.[18,36]

To assess whether Tyr-phosphorylation of ATIC and VASP was regulated by the NPM-ALK, both proteins were immunoprecipitated and analyzed by Western blotting. Figure 3A shows that the down-regulation of NPM-ALK in ALCL cell lines by RNAi coincided with a significant decrease of p-ATIC and p-VASP, whereas their expression remained unaffected. Similarly, treatment of cells with the ALK inhibitor, CEP14083, but not the control CEP11988, led to a significant decrease of p-ATIC and p-VASP (Figure 3B).

Having determined that ATIC and VASP phosphorylation is mediated by ALK, we subsequently investigated their physical association with NPM-ALK. ATIC and VASP coprecipitated with NPM-ALK, and this interaction was largely lost when the expression of NPM-ALK was down-regulated via ALK RNAi (Figure 3C) or, alternatively, when its kinase activity was pharmacologically repressed (Figure 3D).

NPM-ALK enhances ATIC enzymatic activity

To test whether the Tyr-phosphorylation of ATIC modulates its enzymatic activity, we set 3 different assays, determining the transformylase (AICAR-FT), cyclohydrolase (IMP-CHase), and the total ATIC activity. NPM-ALK was enriched by immunoprecipitation using NPM-ALK HEK-293T-Rex cells and then combined in vitro with wild-type-ATIC from HEK-293T. Figure 4A shows that ATIC activity was enhanced in the presence of NPM-ALK, whereas it remained at the basal level when NPM-ALK was inhibited or when an inactive NPM-ALK (NPM-ALK^{K210R}) was used. The finding that ATIC activity was enhanced by its phosphorylation was further demonstrated using lambda-phosphatase capable to dephosphorylate p-ALK species (Figure 4B).

To exclude that the increased activity of ATIC could be the result of the neoplastic phenotype, we measured in parallel the activity of other metabolic enzymes (LDH, G6PD, 6PGD, and ODC). LDH was selected as a control because it was highly phosphorylated in NPM-ALK-positive cells (according to LC-MS/MS data), although it was not modulated by NPM-ALK kinase activity (Figure 5A). Considering that ATIC can be a ALK partner with ATIC-ALK fusion chimera,[9] we stably transfected an ATIC-ALK construct into the HEK-293T-Rex cells and showed that the

Downloaded from http://ashpublications.net/blood/article-pdf/113/12/2776/1305103/zh801209002776.pdf by guest on 20 May 2024

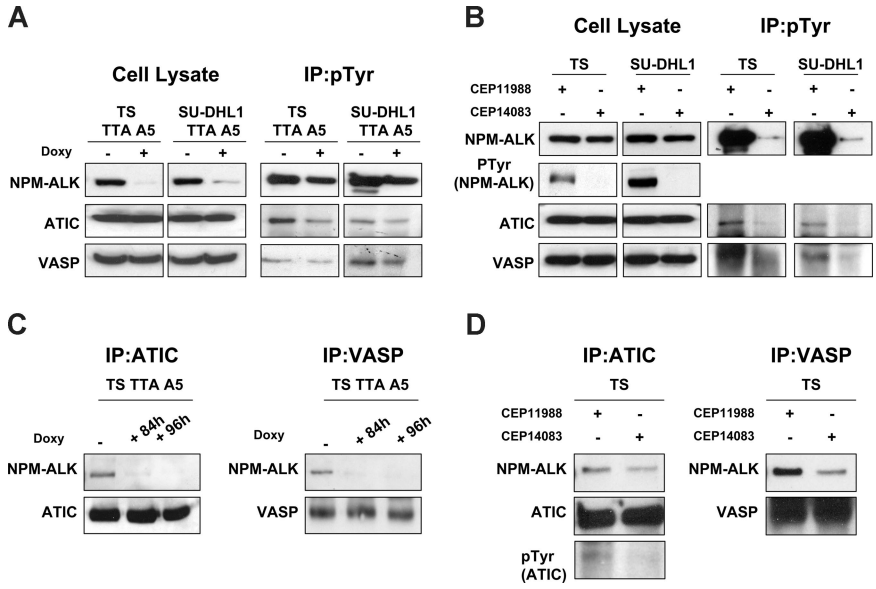

Figure 3. ATIC and VASP phosphorylation is dependent on NPM-ALK kinase activity. (A) Phosphotyrosine containing proteins were first immunoprecipitated (IP) with a specific anti (pTyr) antibody and subsequently blotted with the indicated antibodies. (B) Lysates from ALK$^+$ ALCL cell lines (TS and SU-DHL1), treated with small-molecule ALK inhibitor (CEP14083) or a control compound (CEP11988), were immunoprecipitated and blotted with the indicated antibodies. (C) Total lysates from doxycycline-treated TS TTA A5 cells (1 mg/mL for 84 and 96 hours) were IP with a specific anti-ATIC or anti-VASP antibody and blotted with anti-ALK antibody. (D) Total proteins from TS cells (300 nM of CEP14083 or CEP11988) were IP with a specific anti-ATIC or anti-VASP antibody and blotted with anti-ALK antibody.

wild-type ATIC activity was also enhanced by this fusion, similar to the NPM-ALK chimera (Figure 5B).

Next, to test whether the up-regulation of ATIC activity could be associated with a neoplastic phenotype and/or with other kinases, we transfected the HEK-293T cells with TPR-Met, c-Myc, and Ras expressing constructs. Figure 5C shows that all fusion kinases increased the ATIC activity, but this effect was significantly higher in NPM-ALK and in Ras (RasV12) transfected cells. Because Ras is a downstream target of NPM-ALK,[37] we tested whether it was required in the NPM-ALK–mediated ATIC activation. Figure 5D shows that NPM-ALK–driven activation of ATIC was not affected by a dominant negative Ras construct.

To confirm our findings in a model that mimics human ALCL, we treated ALK$^+$ (SU-DHL1, TS, and JB-6) and ALK$^-$ (Mac-1) ALCL cell lines with CEP14083, and then we evaluated the activity of ATIC and other metabolic enzymes (G6PD and ODC). All enzymatic measurements were performed shortly after the pharmacologic inhibition and in viable cells, as determined by tetramethylrhodamine methyl ester (TMRM) staining. ATIC activity was gradually reduced over a 6-hour time course after CEP14083 treatment in ALK$^+$ cells, whereas no effect was documented in

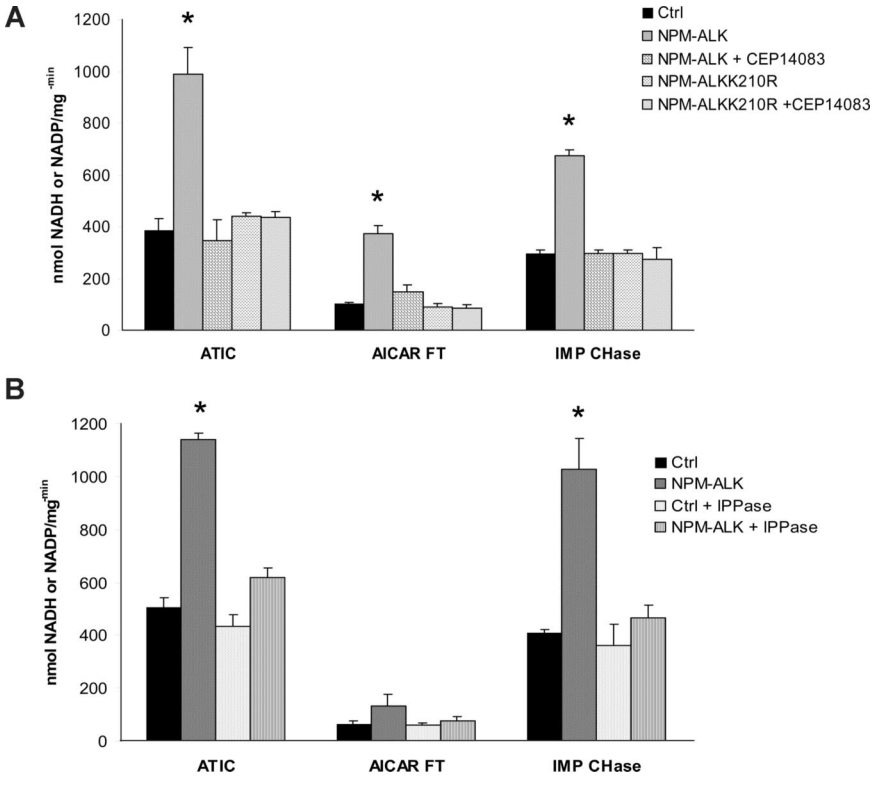

Figure 4. ATIC activity is enhanced in the presence of NPM-ALK in vitro. (A) Immunoprecipitated ATIC was combined with the active NPM-ALK kinase (isolated from wild-type HEK-293T cells and NPM-ALK$^+$ HEK-293T cells, respectively) or with a mutated NPM-ALK^{K210R} kinase (from NPM-ALK^{K210R}–positive HEK-293T cells), with and without the ALK inhibitor CEP14083 (6 hours). Total or specific ATIC activity was measured as described in "Measurement of AICAR-FT/IMP-CHase activity." (B) ATIC enzymatic activities were also determined in the presence of lambda phosphatase (1 mg for 1 hour). *$P < .001$.

Downloaded from http://ashpublications.net/blood/article-pdf/113/12/2776/1305103/zh801209002776.pdf by guest on 20 May 2024

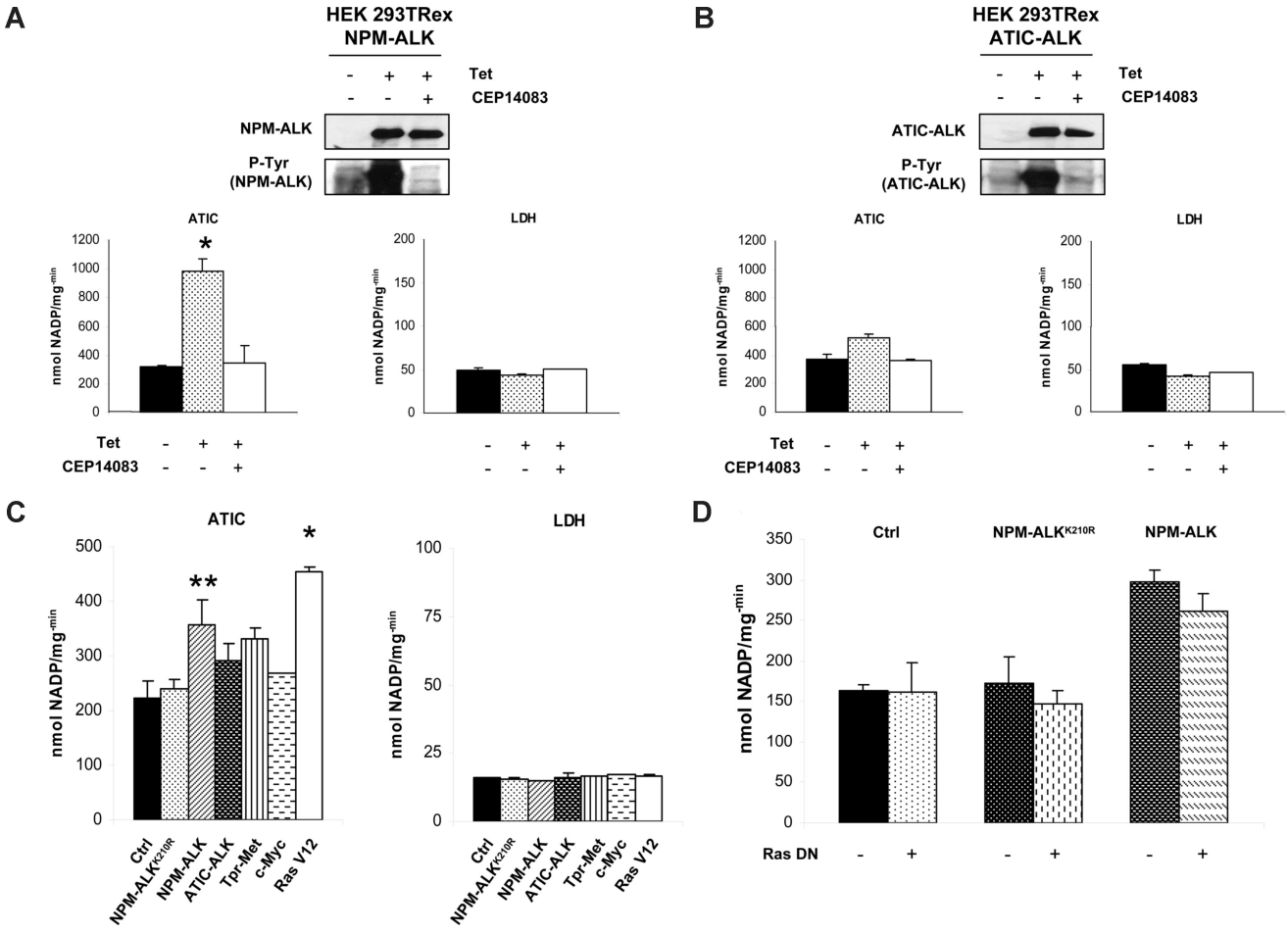

Figure 5. The ATIC activity is enhanced by NPM-ALK in HEK-293T-Rex cells. (A) NPM-ALK inducible HEK-293T-Rex cells were induced with tetracycline with and without CEP14083 ALK inhibitor. p-NPM-ALK was determined by Western blotting using anti–p-ALK antibodies. ATIC and LDH enzymatic activities were evaluated; $^*P < .001$. (B) HEK-293T-Rex cells containing an inducible ATIC-ALK construct were induced with tetracycline and/or with CEP14083. Western blotting analysis confirmed ALK expression and phosphorylation. Enzymatic activity of ATIC and LDH was evaluated. (C) Cell lysates of transiently transfected HEK-293T cells (NPM-ALK, NPM-ALK^{K210R}, ATIC-ALK, TPR-Met, c-myc, and the self-activating form of Ras, Ras V12) were tested for their ATIC and LDH enzymatic activity. $^*P < .001$, $^{**}P < .05$. (D) Cell lysates from transiently transfected HEK-293T cells with NPM-ALK, NPM-ALK^{K210R}, and/or a Ras DN, respectively, were tested for their ATIC and LDH enzymatic activity.

ALK$^-$ cells (Figure 6). Notably, both G6PD and ODC activities remained unaffected under these conditions.

NPM-ALK protects cancer cells from the effects of MTX

To test whether the enzymatic modulation of ALK-mediated ATIC activity could be biologically relevant, we studied ATIC inhibition via MTX, a folic acid analog.[38,39] MTX decreased the ATIC transformylase and the total enzyme activity, whereas its cyclohydrolase function remained unaffected (Figure 7A). In the presence of NPM-ALK, the effect of the MTX was partially abrogated, and higher doses of MTX were required to produce similar inhibitory rates compared with samples lacking NPM-ALK. To demonstrate that the NPM-ALK activity was necessary, we inhibited ALK kinase activity by CEP14083, and this led to a reduced ATIC transformylase activity in the presence of MTX (Figure 7B). Finally, to validate these findings in a cell-based assay, NPM-ALK or NPM-ALK^{K210R} retroviral particles were transduced into T-cell lymphoma cells (CEM). Cells were then treated with the MTX and ATIC activity was determined. ATIC was impaired by MTX, whereas other cellular enzymes (LDH, G6PD, and 6PGD) were not affected (data not shown), either in control or NPM-ALK^{K210R} cells. On the contrary, the inhibition of ATIC by MTX was less pronounced in ALK$^+$ CEM cells (Figure 7C).

Discussion

We used 2 proteomic methods, together with a functional validation approach, to identify novel molecules downstream to NPM-ALK. Performing global HTP posttranscriptional analyses offers a new and powerful approach to dissect pathogenic mechanisms and to apply novel technologies for the diagnosis of malignancy, identification of biomarkers, discovery of targets, and design of tailored therapies.[2-4,40]

We confirmed that ALK signaling is associated with a well-defined transcriptional signature[13,14] and that ALK$^+$ cells preferentially express phosphorylated proteins with specific functions.[10] Our data revealed some proteins in common with those reported in previous HTP proteomic studies and identified new targets.[16,41-43] Relevant proteins were either known mediators of the ALK-signaling or novel proteins, including transcription factors, cytoskeletal/structural, motor/adhesion, and ribosomal proteins or proteins involved in the nucleic acid and/or protein metabolism.

Downloaded from http://ashpublications.net/blood/article-pdf/113/12/2776/1305103/zh801209002776.pdf by guest on 20 May 2024

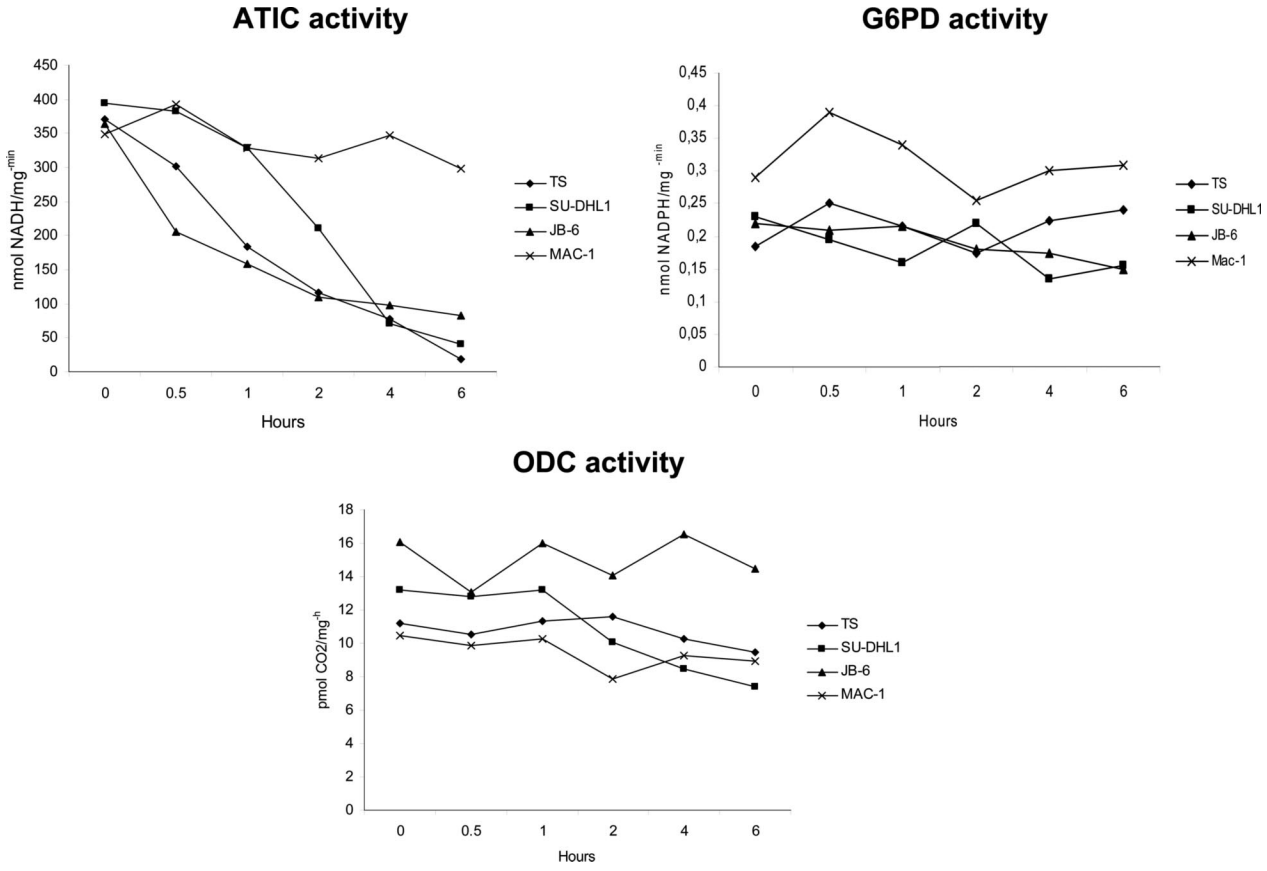

Figure 6. The inhibition of NPM-ALK abrogated the ATIC activity in ALCL cells. The enzymatic activity of ATIC, G6PD, and ODC was measured in ALK$^+$ (TS, SU-DHL1, JB-6) and ALK$^-$ (Mac-1) lymphoblastoid cell lines after treatment with a specific ALK inhibitor, as described in "Measurement of AICAR-FT/IMP-CHase activity."

Proteomic studies are successful tools for the diagnosis of ALCL[42] and for the identification of ALK-related proteins and/or adaptor molecules.[26,44] Our findings are in line with those of Rush et al, who have first demonstrated that HTP proteomics of Tyr-phosphorylated peptides provide selective signatures, identifying key regulators and predicting signaling pathways.[15] Although proteomic studies have unveiled new players within kinase-driven signaling, it is well established that any molecular signature is not fully representative of the tumorigenic events leading to cellular transformation. Indeed, each genetic alteration may be simply associated with a given neoplastic phenotype but may lack any pathogenetic role; these lesions are now referred to as "passengers." Although these defects do not maintain the neoplastic phenotype, they often represent "tumor-associated biomarkers" capable of better stratifying tumors or patients allowing better patient follow-up during treatment. Pathogenetically relevant lesions, referred to as "drivers," have a more pertinent impact and represent ideal targets for novel therapies. Thus, it has become imperative to design strategies dissecting "passengers" from "drivers."

Although proteomic approaches may be more informative than genomic analyses, functional validation studies are required to dissect the relationships between causal events and phenotypes and to define the tumorigenic contribution of each change.

Because HTP analyses are often descriptive, we adopted 2 alternative strategies to gain more insights into ALK-mediated transformation. First, we have compared the phospho-profile obtained from ALK$^+$ ALCL cell lines with those derived from cells ectopically expressing ALK fusions, in the presence or in the absence of ALK signaling. These models have revealed a restricted set of phosphoproteins shared by ALK cells, in different cellular contexts. Although this may be restrictive and could result in the loss of relevant ALK-associated targets, it defines a limited number of proteins, whose phosphorylation status is highly reproducible and strictly dependent on ALK signaling. Second, to identify a biologically relevant set of ALK-associated proteins, we used an ALK inhibitor and performed a quantitative determination of phosphorylation changes. These studies have shown that determining the level of protein phosphorylation is necessary to identify appropriate targets, many of them undetectable using semiquantitative approaches.

To validate newly defined ALK-associated proteins, we performed biochemical studies, which confirmed that VASP and ATIC were associated with NPM-ALK and phosphorylated. More importantly, we demonstrated that ATIC phosphorylation enhanced its enzymatic activity. This is the first demonstration that ALK-mediated phosphorylation leads to an enhanced metabolic activity of a substrate, which may contribute to cell transformation. Enhanced purine synthesis sustains cell proliferation, and its therapeutic inhibition has been adopted to hamper tumor growth in many human malignancies. The discovery that ALK posttranscriptional modifications may change the activity of a key enzyme is important because this observation may be applied to other kinase-driven tumors. This hypothesis is supported by the detection of p-ATIC in many tumor cell lines and fresh samples.[18,36] Thus, it is tempting to speculate that the detection of p-ATIC may be useful to predict the response to antifolate agents and facilitate the design of more efficacious therapeutic protocols. The identification of tumorigenic molecules has served as a platform to improve chemotherapeutic protocols using conventional cancer agents and to open a new era in anticancer research in which new targeted compounds are being developed to supplant the more toxic traditional anticancer drugs.

Downloaded from http://ashpublications.net/blood/article-pdf/113/12/2776/1305103/zh801209002776.pdf by guest on 20 May 2024

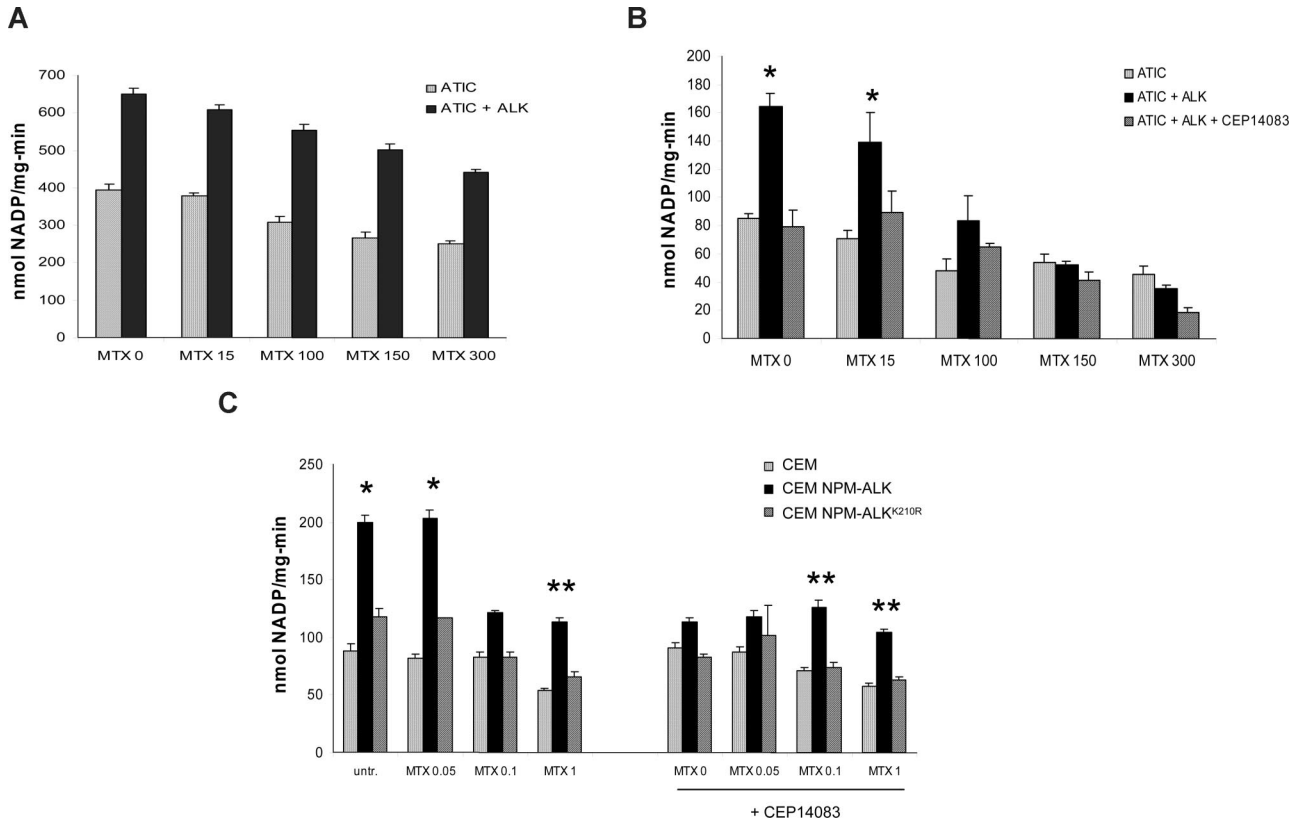

Figure 7. NPM-ALK attenuates the effect of methotrexate in lymphoma cells. (A) ATIC enzyme and NPM-ALK kinase were immunoprecipitated from 2 mg of HEK-293T cell lysates and then combined in vitro with increasing concentrations of MTX. Enzymatic activity of total ATIC was measured in vitro. $P < .005$. (B) ATIC enzyme and NPM-ALK kinase were combined in vitro in the presence of increasing concentrations of MTX and 300 nM of CEP14083 and AICAR-FT activity was measured. *$P < .05$. (C) CCRF-CEM cells were infected with NPM-ALK or the kinase dead mutant NPM-ALK^{K210R} and treated in culture with increasing concentrations of MTX for 24 hours. Where indicated, the cells were pretreated with 300 nM of CEP14083 for 30 minutes before MTX treatment. AICAR-FT activity was measured. *$P < .001$, **$P < .005$.

Here we provided new evidence on a posttranscriptional modification of a key purine synthesis enzyme, which may predict response to antifolate analogs. Detailed knowledge of ATIC enzyme activity in human tumors may allow the identification of low responders and thus the application of ad hoc therapeutic strategies or patient-related dose regimens.

Acknowledgments

The authors thank Drs Paola Bernabei and Andrea Manazza for their technical help and management the flow cytometry and image cores.

This work was supported in part by the National Institutes of Health (Bethesda, MD; R01-CA90773), the Sixth Research Framework Programme of the European Union, Project RIGHT (LSHB-CT-2004-005276), Ministero dell'Università e Ricerca Scientifica, Regione Piemonte, Compagnia di San Paolo, Torino (Progetto Oncologia), Associazione Italiana per la Ricerca sul Cancro and Fondazione Guido Berlucchi. C.V. was supported by a fellowship from the Fondazione Italiana per la Ricerca sul Cancro (FIRC, Milano, Italy). F.E.B. is the recipient of a Research Fellowship from the Fondazione Internazionale di Ricerca in Medicina Sperimentale (FIRMS, Torino, Italy).

Authorship

Contribution: C.V., R.D.P., R.C., A.B., M.J.C., and G.I. designed research; F.E.B., C.R., L.D., L.R., and V.L.G. performed research; M.C., B.R., J.R., and O.N.J. contributed reagents/analytic tools; K.L. and J.N. analyzed and interpreted data; and F.E.B., C.V., and G.I. wrote the paper.

Conflict-of-interest disclosure: G.I. receives research support from Cephalon. The remaining authors declare no competing financial interests.

Correspondence: Giorgio Inghirami, Center for Experimental Research and Medical Studies, Department of Biomedical Sciences and Human Oncology, University of Torino, Via Santena 5, 10126 Torino, Italy; e-mail: giorgio.inghirami@unito.it.

References

1. Hanahan D, Weinberg RA. The hallmarks of cancer. Cell. 2000;100:57-70.
2. Chen P, Schulze-Gahmen U, Stura EA, et al. Crystal structure of glycinamide ribonucleotide transformylase from Escherichia coli at 3.0 A resolution: a target enzyme for chemotherapy. J Mol Biol. 1992;227:283-292.
3. Rayl EA, Moroson BA, Beardsley GP. The human purH gene product, 5-aminoimidazole-4-carboxamide ribonucleotide formyltransferase/IMP cyclohydrolase: cloning, sequencing, expression, purification, kinetic analysis, and domain mapping. J Biol Chem. 1996;271:2225-2233.
4. Beardsley GP, Rayl EA, Gunn K, et al. Structure and functional relationships in human pur H. Adv Exp Med Biol. 1998;431:221-226.
5. Vergis JM, Bulock KG, Fleming KG, Beardsley GP. Human 5-aminoimidazole-4-carboxamide ribonucleotide transformylase/inosine 5′-monophosphate cyclohydrolase: a bifunctional protein requiring dimerization for transformylase activity but not for cyclohydrolase activity. J Biol Chem. 2001;276:7727-7733.
6. Reyes VM, Greasley SE, Stura EA, Beardsley GP, Wilson IA. Crystallization and preliminary crystallographic investigations of avian 5-aminoimi-

Downloaded from http://ashpublications.net/blood/article-pdf/113/12/2776/1305103/zh801209002776.pdf by guest on 20 May 2024

dazole-4-carboxamide ribonucleotide transformylase-inosine monophosphate cyclohydrolase expressed in Escherichia coli. Acta Crystallogr D Biol Crystallogr. 2000;56:1051-1054.

7. Colleoni GW, Bridge JA, Garicochea B, Liu J, Filippa DA, Ladanyi M. ATIC-ALK: a novel variant ALK gene fusion in anaplastic large cell lymphoma resulting from the recurrent cryptic chromosomal inversion, inv(2)(p23q35). Am J Pathol. 2000;156:781-789.
8. Ma Z, Cools J, Marynen P, et al. Inv(2)(p23q35) in anaplastic large-cell lymphoma induces constitutive anaplastic lymphoma kinase (ALK) tyrosine kinase activation by fusion to ATIC, an enzyme involved in purine nucleotide biosynthesis. Blood. 2000;95:2144-2149.
9. Trinei M, Lanfrancone L, Campo E, et al. A new variant anaplastic lymphoma kinase (ALK)-fusion protein (ATIC-ALK) in a case of ALK-positive anaplastic large cell lymphoma. Cancer Res. 2000; 60:793-798.
10. Chiarle R, Voena C, Ambrogio C, Piva R, Inghirami G. The anaplastic lymphoma kinase in the pathogenesis of cancer. Nat Rev Cancer. 2008;8:11-23.
11. Piva R, Chiarle R, Manazza AD, et al. Ablation of oncogenic ALK is a viable therapeutic approach for anaplastic large-cell lymphomas. Blood. 2006; 107:689-697.
12. Galkin AV, Melnick JS, Kim S, et al. Identification of NVP-TAE684, a potent, selective, and efficacious inhibitor of NPM-ALK. Proc Natl Acad Sci U S A. 2007;104:270-275.
13. Piva R, Pellegrino E, Mattioli M, et al. Functional validation of the anaplastic lymphoma kinase signature identifies CEBPB and BCL2A1 as critical target genes. J Clin Invest. 2006;116:3171-3182.
14. Lamant L, de Reynies A, Duplantier MM, et al. Gene-expression profiling of systemic anaplastic large-cell lymphoma reveals differences based on ALK status and two distinct morphologic ALK+ subtypes. Blood. 2007;109:2156-2164.
15. Rush J, Moritz A, Lee KA, et al. Immunoaffinity profiling of tyrosine phosphorylation in cancer cells. Nat Biotechnol. 2005;23:94-101.
16. Sjostrom C, Seiler C, Crockett DK, Tripp SR, Elenitoba Johnson KS, Lim MS. Global proteome profiling of NPM/ALK-positive anaplastic large cell lymphoma. Exp Hematol. 2007;35:1240-1248.
17. Goss VL, Lee KA, Moritz A, et al. A common phosphotyrosine signature for the Bcr-Abl kinase. Blood. 2006;107:4888-4897.
18. Rikova K, Guo A, Zeng Q, et al. Global survey of phosphotyrosine signaling identifies oncogenic kinases in lung cancer. Cell. 2007;131:1190-1203.
19. Walters DK, Goss VL, Stoffregen EP, et al. Phosphoproteomic analysis of AML cell lines identifies leukemic oncogenes. Leuk Res. 2006;30:1097-1104.
20. Guo A, Villen J, Kornhauser J, et al. Signaling networks assembled by oncogenic EGFR and c-Met. Proc Natl Acad Sci U S A. 2008;105:692-697.
21. Zamo A, Chiarle R, Piva R, et al. Anaplastic lymphoma kinase (ALK) activates Stat3 and protects hematopoietic cells from cell death. Oncogene. 2002;21:1038-1047.
22. Ambrogio C, Voena C, Manazza AD, et al. p130Cas mediates the transforming properties of the anaplastic lymphoma kinase. Blood. 2005; 106:3907-3916.
23. Wan W, Albom MS, Lu L, et al. Anaplastic lymphoma kinase activity is essential for the proliferation and survival of anaplastic large-cell lymphoma cells. Blood. 2006;107:1617-1623.
24. Ong SE, Blagoev B, Kratchmarova I, et al. Stable isotope labeling by amino acids in cell culture, SILAC, as a simple and accurate approach to expression proteomics. Mol Cell Proteomics. 2002; 1:376-386.
25. Gruhler A, Olsen JV, Mohammed S, et al. Quantitative phosphoproteomics applied to the yeast pheromone signaling pathway. Mol Cell Proteomics. 2005;4:310-327.
26. Voena C, Conte C, Ambrogio C, et al. The tyrosine phosphatase Shp2 interacts with NPM-ALK and regulates anaplastic lymphoma cell growth and migration. Cancer Res. 2007;67: 4278-4286.
27. Uyeda K, Rabinowitz JC. Fluorescence properties of tetrahydrofolate and related compounds. Anal Biochem. 1963;6:100-108.
28. Suormala T, Gamse G, Fowler B. 5,10-Methylenetetrahydrofolate reductase (MTHFR) assay in the forward direction: residual activity in MTHFR deficiency. Clin Chem. 2002;48:835-843.
29. Digits JA, Hedstrom L. Species-specific inhibition of inosine 5′-monophosphate dehydrogenase by mycophenolic acid. Biochemistry. 1999;38: 15388-15397.
30. Flaks JG, Erwin MJ, Buchanan JM. Biosynthesis of the purines: XVI. The synthesis of adenosine 5′-phosphate and 5-amino-4-imidazolecarboxamide ribotide by a nucleotide pyrophosphorylase. J Biol Chem. 1957;228:201-213.
31. Riganti C, Gazzano E, Polimeni M, Costamagna C, Bosia A, Ghigo D. Diphenyleneiodonium inhibits the cell redox metabolism and induces oxidative stress. J Biol Chem. 2004;279:47726-47731.
32. Farrar WL, Harel-Bellan A. Myeloid growth factor(s) regulation of ornithine decarboxylase: effects of antiproliferative signals interferon-gamma and cAMP. Blood. 1989;73:1468-1475.
33. Miyake I, Hakomori Y, Shinohara A, et al. Activation of anaplastic lymphoma kinase is responsible for hyperphosphorylation of ShcC in neuroblastoma cell lines. Oncogene. 2002;21:5823-5834.
34. Wentworth JK, Pula G, Poole AW. Vasodilator-stimulated phosphoprotein (VASP) is phosphorylated on Ser157 by protein kinase C-dependent and -independent mechanisms in thrombin-stimulated human platelets. Biochem J. 2006;393:555-564.
35. Anderson DC, Li W, Payan DG, Noble WS. A new algorithm for the evaluation of shotgun peptide sequencing in proteomics: support vector machine classification of peptide MS/MS spectra and SEQUEST scores. J Proteome Res. 2003;2: 137-146.
36. Gu TL, Goss VL, Reeves C, et al. Phosphotyrosine profiling identifies the KG-1 cell line as a model for the study of FGFR1 fusions in acute myeloid leukemia. Blood. 2006;108:4202-4204.
37. Turner SD, Yeung D, Hadfield K, Cook SJ, Alexander DR. The NPM-ALK tyrosine kinase mimics TCR signalling pathways, inducing NFAT and AP-1 by RAS-dependent mechanisms. Cell Signal. 2007;19:740-747.
38. Allegra CJ, Drake JC, Jolivet J, Chabner BA. Inhibition of phosphoribosylaminoimidazole-carboxamide transformylase by methotrexate and dihydrofolic acid polyglutamates. Proc Natl Acad Sci U S A. 1985;82:4881-4885.
39. Budzik GP, Colletti LM, Faltynek CR. Effects of methotrexate on nucleotide pools in normal human T cells and the CEM T cell line. Life Sci. 2000;66:2297-2307.
40. Cho WC. Contribution of oncoproteomics to cancer biomarker discovery. Mol Cancer. 2007;6:25.
41. Crockett DK, Lin Z, Elenitoba-Johnson KS, Lim MS. Identification of NPM-ALK interacting proteins by tandem mass spectrometry. Oncogene. 2004;23:2617-2629.
42. Elenitoba-Johnson KS, Crockett DK, Schumacher JA, et al. Proteomic identification of oncogenic chromosomal translocation partners encoding chimeric anaplastic lymphoma kinase fusion proteins. Proc Natl Acad Sci U S A. 2006; 103:7402-7407.
43. Cussac D, Pichereaux C, Colomba A, et al. Proteomic analysis of anaplastic lymphoma cell lines: identification of potential tumor markers. Proteomics. 2006;6:3210-3222.
44. Lim MS, Elenitoba-Johnson KS. Mass spectrometry-based proteomic studies of human anaplastic large cell lymphoma. Mol Cell Proteomics. 2006;5:1787-1798.

Downloaded from http://ashpublications.net/blood/article-pdf/113/12/2776/1305103/zh801209002776.pdf by guest on 20 May 2024